Analytica Chimica Acta 1355 (2025) 344026

Contents lists available at ScienceDirect

Analytica Chimica Acta

journal homepage: www.elsevier.com/locate/aca

Chemical fingerprint of bacteriophages by infrared nano-spectroscopy

Yue Cao [a,1], Dipesh Khanal [a,*,1], Adrian Cernescu [b], Hak Kim Chan [a,**]

[a] Advanced Drug Delivery Group, Sydney Pharmacy School, Faculty of Medicine and Health, The University of Sydney, NSW, 2006, Australia
[b] Attocube Systems AG, Eglfinger Weg 2, Haar, D-85540, Munich, Germany

HIGHLIGHTS

- Bacteriophages are nanoscale antimicrobial agents with selective bacterial targeting.
- Significant heterogeneity exists in phage morphology and chemical composition.
- s-SNOM provides a label-free mapping of phage chemical composition at the nanoscale.
- Contributes to building a comprehensive reference library of phage chemical and morphological composition profiles.
- Enable optimization of phage formulations, improving their stability and effectiveness as therapeutic agents.

GRAPHICAL ABSTRACT

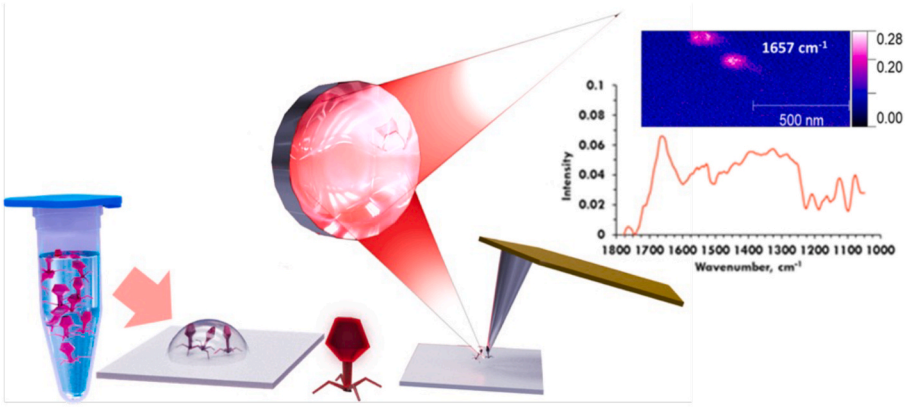

ARTICLE INFO

Handling Editor: Xiu-Ping Yan

Keywords:
Bacteriophage (phage)
Nano-chemical mapping
Spectroscopy
AFM
Phage stability
Phage formulation
Pseudomonas aeruginosa

ABSTRACT

Bacteriophage (phages) are naturally occurring nanoscale antimicrobial agents that can self-replicate at infection sites and selectively eliminate pathogenic bacteria. Significant heterogeneity exists in phage properties such as morphology, protein and nucleic acid composition, subject to the strain, state, and environment of the phage source. However, current techniques fall short in accurately mapping the chemical compositions of individual phages. A thorough understanding of this heterogeneity is essential to elucidate the difference between phage types and their stability, which may impact phages as effective therapeutic agents. We propose using scattering scanning near-field optical microscopy (s-SNOM) as an innovative method to map the chemical composition of phages at the nanoscale. The strength of this method lies in its label-free, ultra-high sensitivity that measures individual phage chemical heterogeneity. Additionally, s-SNOM is ideal for thermally sensitive phages, as it detects light scattered by nanoscale specimens without relying on thermal expansion. New insights from this method into phage chemical composition will profoundly impact our understanding of phage biology and optimise phage formulation for therapeutic use.

* Corresponding author.
** Corresponding author.
E-mail addresses: dipesh.khanal@sydney.edu.au (D. Khanal), kim.chan@sydney.edu.au (H.K. Chan).
[1] Authors contributed equally.

https://doi.org/10.1016/j.aca.2025.344026
Received 8 December 2024; Received in revised form 2 April 2025; Accepted 4 April 2025
Available online 4 April 2025

1. Introduction

Bacteriophages (phages) are natural nanoscale antimicrobial agents that selectively target and destroy pathogenic bacteria [1,2]. Phages play a critical role in our ecosystem, by potentially reducing 10–80 % of environmental bacterial populations. It is important to also mention that phage particles are complex viruses that are composed of nucleic acid in the form of double or single-stranded RNA/DNA encased in a protein capsid. Several phage types also have long tails, which are made of proteins [3]. Lipid components may exist in some phage structures as well [4].

Phages have been successfully applied in treating bacterial infections affecting the skin [5], and respiratory tract [1] among many others [6]. In addition to therapeutic applications, phages have been incorporated into biocontrol formulations. However, many of these formulations, typically protein-based, lack fundamental chemical insights. The absence of this chemical knowledge impedes the development of stable effective phage formulations, affecting the outcome of clinical trials [7]. To improve existing applications of phages and to enable novel ones, a thorough understanding of these viruses is required.

Electron microscopy [8] and wet chemical methods such as gel electrophoresis [9] and mass spectrometry [10], are commonly used to evaluate phage morphology and analyse genomic and protein heterogeneity. However, these applications are time- and labour-consuming and the knowledge often derives from bulk measurements of phage populations, providing limited details on individual phages. Traditional Fourier Transform Infrared Spectroscopy (FTIR) and Raman spectroscopy, constrained by diffraction boundaries, fail to evaluate the chemical composition of individual phages effectively, achieving spatial resolutions between 1.5 and 10 μm for IR and 250–500 nm for Raman. While valuable, wet chemical methods yield only averaged chemical data for the phage populations and spectra measurements using bulk FTIR may not be able to represent the chemical fingerprint of the sample at the nano level, such as the phages of interest here, which are typically less than 200 nm in size. Hence, it would be challenging to use these methods to analyse phages at an individual level.

Understanding the physical and chemical properties of individual phages is crucial for deciphering their degradation, destabilisation, or stabilisation in formulation development. Scattering scanning near-field optical microscopy (s-SNOM) overcomes the limitations of traditional spectroscopic and wet chemical methods. Similar to tip-enhanced Raman spectroscopy (TERS), s-SNOM uses a metallic tip to probe molecular vibrations for chemical imaging and nanoscale IR spectra acquisition by Fourier transforming the scattered light from the specimen after tip illumination by a broadband infrared laser. S-SNOM, using an atomic force microscopy (AFM) tip offers ultrahigh resolution and sensitivity by merging the high spatial resolution of atomic force microscopy (AFM) imaging with spectroscopy to achieve resolutions (around 20 nm) well below the detection limit of conventional IR spectroscopy. As a novel spectroscopy technique, nano-FTIR has been pivotal in several multidisciplinary investigations such as nano-mapping of individual protein complexes [11], nano-chemistry of multi-phase bio-minerals [12] and nano-heterogeneity of polymer blends [13,14].

IR spectroscopy analysis faces challenges with biological substances with weak scattering capabilities compared to polar crystals. To overcome this, several innovative techniques have been developed to explore the sub-wavelength organic chemistry of materials, including local thermal expansion [15–17] and synchrotron AFM-IR [18]. Our previous study utilised photothermal-induced resonance-enhanced AFM-IR to detect phages and display their protein conformations [19]. The samples were examined using the top-down illumination, and only one type of phage was characterised after being formulated into aerosol powder. This technique detects local expansions or temperature rise with an AFM tip following IR absorption by a sample, enhancing the sensitivity to organic vibrational resonances and providing clearer data interpretation. However, in thermal expansion microscopy, spatial resolution is limited by the uncontrolled diffusion of beam power into the material, complicating the analysis [20].

In nano-FTIR, the resolution of the optical probe is solely determined by the radius of the AFM tip, enabling these methods to uniquely conduct ultra-broadband IR spectroscopy at a resolution of 25 nm. We previously evaluated three phages using s-SNOM to understand their conformational changes pre- and post-exposure to various organic solvents. This technique, employing tapping mode, revealed structural alterations and highlighted the conformational changes in the secondary structures of phages, aiding in interpreting the solvent-induced inactivation process of phages. However, the chemical mapping at certain wavelengths was not evaluated. This experiment aimed to evaluate the effectiveness of nano-FTIR in the nanochemical analysis of different types of phages. Nano-FTIR offers exceptional resolution for identifying phage distributions in minimal quantities, yet locating these nanoscale phages remains challenging. This challenge is surmountable by initially scanning larger sample sections and subsequently performing chemical imaging at phage-specific wavenumbers, enabling identification of phage-containing regions. Zooming into individual particles further permits high-resolution spectral acquisition and chemical mapping. A significant research gap exists in the chemical characterisation of nanosized phages with the nano-FTIR technique.

Chemical imaging at the nanoscale is beneficial in resolving spatial heterogeneities in phages, which may not be possible without using point spectroscopy, i.e., collecting spectra at different locations within the phage structure. In this study, we employed a combination of transmission electron microscopy (TEM) and nanochemical imaging using nano-FTIR to probe the morphological features and spatial distribution of proteins and nucleic acids of *Pseudomonas aeruginosa*-specific phages.

2. Materials and methods

2.1. Bacteriophage purification and plaque assay

Two *Pseudomonas aeruginosa* phages, consisting of podovirus (PEV31), and myovirus (PEV20), were isolated from the sewage treatment plant in Olympia (WA, USA) by the Kutter Lab (Evergreen Phage Lab). The isolation used *P. aeruginosa* dog-ear strain PAV237, which also served as the host for phage titre assessment. Amplified phages were filtered through a 0.22 μm polyethersulfone (PES) syringe filter (Merck, Germany). The filtered lysates were treated with 10 μg/mL DNase and RNase (Merck, Germany) and incubated at 37 °C for 30 min. DNase and RNase were removed by ultrafiltration at 4000×*g*, at 4 °C using the Allegra X–30R benchtop centrifuge (Beckman Coulter, USA) and samples resuspended in phosphate-buffered saline (PBS) (0.01 M phosphate buffer, 0.0027 M KCl, and 0.137 M NaCl), with pH adjusted to 7.2. EndoTrap®HD (Lionex GmbH, Germany) was employed to remove endotoxins from the phages before purification with an anion-exchange (AEX) column. The optimised AEX process and buffer concentrations for eluting the purest phage fractions were determined previously. The entrapped phages were introduced into the CIMmultus™ diethylamine (DEAE) 2 μm column (BIA Separations, Slovenia) and eluted according to the manufacturer's protocol, with a NaCl concentration unique to each phage. The purest fraction was then cleaned up of endotoxins by a final run with the EndoTrap®HD. The endotoxin levels were quantified by ToxinSensor™ chromogenic Limulus amebocyte lysate assay kit (GenScript, USA). The final phages were stored in PBS with high titres of 10^{10} PFU/mL (see Fig. 1).

The phage concentration was determined by using a plaque assay (Fig. 2). The top-agar layer was prepared by combining overnight culture of the *P. aeruginosa* reference strain with 5 mL of 0.4 % nutrient broth top agar and overlaying onto a 1.5 % nutrient agar plate. Serial dilutions of the phage samples were prepared in a 96-well plate and were done by adding 20 μL samples to 180 μL PBS. From the set of dilutions, 10 μL drops were spotted on the top agar plate, left to dry for 20

min and plates incubated overnight at 37 °C. Following incubation, the plaques forming units were counted to determine the phage titres.

2.2. TEM

TEM assessed the structure and morphology of phage samples.Observations were conducted using an FEI Tecnai T12 microscope (FEI, USA) at 120 kV fitted with a 4k x 4k CCD camera. All samples underwent negative staining on the grid prior to insertion into the instrument for observation. The carbon-coated copper grids (GSCU150CC-50, Proscitech, Australia) were glow-discharged to eliminate residual hydrocarbons and reduce hydrophobicity. The staining procedure began by placing separate 10 μL drops of the sample, 2 % w/v uranyl acetate and Milli-Q water separately side by side on a piece of parafilm. The cleaned grid was placed on the sample drop for 2 min. The excess sample was blotted off with filter paper before transferring the grid to the stain drop for 10 s. Excess stain was removed with absorbent filter paper, then the grid was placed on the water drop for 10 s. Following water removal, the grid was air-dried for 3 min before being inserted into the microscope.

2.3. Phage lysate

A 1:10 dilution of phage suspension in ultrapure water (5 μL) was deposited onto a silicon substrate for 3 min. The excess liquid was then removed, and the surface was allowed to dry for 5 min. The samples were scanned in tapping mode.

2.4. Nano-FTIR spectroscopy

The chemical characterisation of each phage type was conducted using nano-FTIR spectroscopy, *IR*-neaSCOPE $^{+\,s}$ (Neaspec, Germany), which combines the analytical power of FTIR spectroscopy with the nanoscale spatial resolution of AFM. IR spectra were collected at a resolution of 4 cm^{-1}, using a scattering-type near-field optical microscope (neaSNOM, attocube systems AG), equipped with a broadband Difference Frequency Generation (DFG) laser source (Toptica Photonics AG) and an asymmetric Michelson interferometer. A PtIr tip with ca. 20 nm diameter (nanoworld, Switzerland) probed the sample in intermittent contact mode at the frequency Ω of *ca.* 250 kHz, modulating the intensity of the scattered IR light at Ω and its higher harmonics. Demodulation at a higher harmonic nΩ of Ω distinguishes the near-field optical signal from the background signal [11,21]. The instrumental response function was removed from the nano-FTIR spectra by normalizing the measured spectra against a reference Si signal. This resulted in nano-FTIR Absorption and Reflectivity spectra directly correlatable with the standard far-field IR spectra [22]. AFM images of each phage type were obtained, with multiple IR point spectra acquired from both the head and the tail. Data analysis was performed using neaPLOT software. A minimum of 20–30 phages were analyzed.

Before data acquisition, spectral calibration was conducted using a polystyrene standard. Tip sharpness and intactness were validated by imaging standard grids and verified by accurate sample topography tracking. These evaluations collectively ensured optimal functionality of nano-FTIR system, providing confidence in the reliability of our phage analysis results.

3. Results and discussion

The structural and compositional differences between PEV31 and PEV20 phages were analyzed using a combination of advanced imaging and nanospectroscopic techniques, providing nanoscale insights into their morphology and biochemical organization. TEM imaging (Fig. 2a) reveals the intact morphology of PEV31, characterized by an icosahedral capsid measuring 65 nm and a short, thin, non-contractile tail approximately 10 nm in length. Tapping-mode AFM images (Fig. 2b and d) of drop-casted PEV31 confirm the presence of fully intact phages, with clearly visible heads attached to short tails. Nano-FTIR spectra collected from the capsid region (red, green and grey squares) reveal peaks at 1720 cm^{-1} (nucleic acid), 1660 cm^{-1} (amide I), and ~1550 cm^{-1} (amide II), alongside features at ~1250 and 1060 cm^{-1} attributed to phosphate backbone vibrations (Fig. 2c) [23,24]. These findings suggest a tightly packed capsid structure rich in nucleic acids and proteins.

In contrast, TEM imaging (Fig. 3a) shows that PEV20 has an icosahedral capsid of similar size (60–65 nm) but is distinguished by a long, straight contractile tail measuring 120–125 nm. AFM height imaging corroborates these observations by capturing its intricate architecture (Fig. 3b and d). Nano-FTIR spectra from the tail (green squares) and head (red and grey squares) regions reveal prominent peaks at ~1650 cm^{-1} (amide I), and ~1550 cm^{-1} (amide II). A shoulder beyond ~1720 cm^{-1} indicative of strong nucleic acid signals from the capsid region (Fig. 3c) [23]. Additional peaks at ~1260 and 1100 cm^{-1} further confirm nucleic acid phosphate backbone contributions (Fig. 3c) [24]. Nano-FTIR spectra from the tail (green squares) and head (red and grey squares) regions reveal prominent peaks at ~1650 cm^{-1} (amide I) and ~1550 cm^{-1} (amide II). A shoulder beyond 1720 cm^{-1} indicates strong nucleic acid signals from the capsid region (Fig. 3c) [23]. To ensure consistency and minimize ambiguity, we collected multiple spectra across different sample regions and the spectral range from 1800 to 1000 cm^{-1}, capturing a broader molecular signature. Notably, additional peaks at 1250 cm^{-1} and 1060 cm^{-1} for PEV31, as well as ~1260 cm^{-1} and ~1100 cm^{-1} for PEV20, were consistently observed. These findings support the assignment of the ~1720 cm^{-1} signal to nucleic acid content and underscore the reproducibility of the spectral analysis. Optical amplitude imaging enhances these analyses by providing

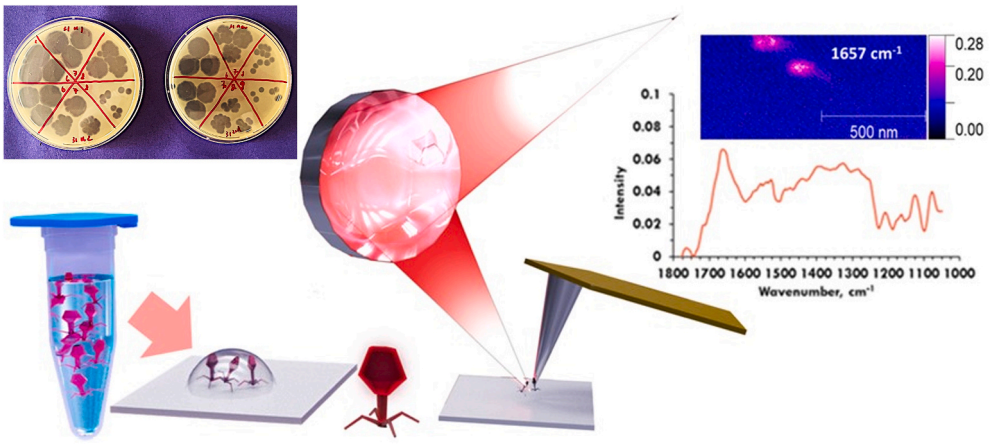

Fig. 1. Illustrative representation of the process and analysis for phage samples using s-SNOM measurement techniques.

spatially resolved contrasts in material composition across both phages (Figs. 2e and 3e) [25]. Together, these findings align with previous studies [3,24], highlighting nano-FTIR's capability to resolve nanoscale biochemical heterogeneity with high spatial precision.

Phage capsids primarily consist of stable protein capsules that enclose genetic materials [26]. The icosahedral capsids of the PEV20 and PEV31 phages in this study are composed of capsomers made of major capsid proteins [27,28]. The stability of major capsid proteins is maintained by electrostatic interactions among charged secondary structures (such as α-helix and β-sheets), embedded in different protein domains of the capsomers. Different phages carry various proportions of secondary structures [29]. Nanochemical information previously obtained from individual point spectra [30] provided insights into the chemical compositions of phages at discrete spatial locations, yet it did not resolve the spatial distribution of proteins and nucleic acids across the entire phage structure. This limitation can be overcome by acquiring nanochemical maps at targeted wavenumbers (e.g., protein-specific amide I/II bands or nucleic acid phosphate vibrations), which would reveal the spatial distribution of these biomolecules across the phage structure.

To evaluate the distribution of protein in PEV31 and PEV20, we collected chemical maps at 1657 cm^{-1}, corresponding to protein structures in phages, for both phages (Figs. 2f and 3f), and an additional chemical map at 1720 cm^{-1} for PEV20, corresponding to nucleic acids (Fig. 3g). The chemical maps at 1657 cm^{-1} highlighted the distribution of protein across the PEV 20 and PEV 31 phages. For PEV20, the condensed, red-coloured regions in the chemical image at 1657 cm^{-1} correspond to the areas with concentrated protein structures within the phage particles. The additional chemical map collected at 1720 cm^{-1} specifically identifies nucleic acid distribution within PEV20. At this wavenumber, the bright, purple-coloured regions in the image correspond to the regions of maximum nucleic acid concentration, facilitating clear visualization of the phage capsid structure.

Overall, our findings confirm that the phages are present with complex protein secondary structures encasing nucleic acid in their capsid. Specifically, the contrast in the image illustrates the chemical composition of the phage sample, highlighting the sensitivity of nano-FTIR in detecting and differentiating molecular variation in phages, thus showcasing the precision of nano-FTIR in revealing the complex biochemical landscape within phage samples [31]. We anticipate that nano-FTIR analysis of phages will advance the study of protein conformations under various environmental conditions, revealing the influence of previously indistinguishable chemical and physical surface heterogeneities. This method will benefit from ongoing improvements in scanning probe microscopy. We expect that modifications to this technique will allow observation of bacterial defence mechanisms against phage infection, enhancing our understanding of phage-host interactions and potentially leading to more effective phage-based therapies. Phages are gaining increasing interest in medical, industrial, and molecular settings [32,33]. Such insights are particularly valuable in phage therapy, where precise chemical profiles can potentially guide the selection or engineering of phages to effectively target specific bacterial surface sites and receptors, including antibiotic-resistant strains [34].

Nano-FTIR also plays a key role in ensuring the consistency, purity, and safety of phage formulations, as it is important for purified phage stocks to be free from bacteria, debris, and bacterial endotoxins [35]. Many unwanted bacterial contaminants, such as outer membrane vesicles, are at nanoscale. By mapping the nanochemical composition phage samples and identifying impurities or unwanted contaminants, nano-FTIR can ensure phage formulations are consistent and contaminant-free, which is critical for meeting regulatory requirements [36,37]. In addition, as more phage profiles are developed, they contribute to a growing library that serves as a reference source for researchers and regulators. The phage profile can facilitate the assessment of new phage formulations and help establish regulatory standards, ensuring the safe and effective use of phage-based therapies.

3.1. Limitations and recommendations

Despite its effectiveness as a powerful tool for nanoscale chemical analysis, nano-FTIR has certain limitations, particularly when applied to biological samples. The requirement for dry samples can compromise the native state of biologics like phages, as drying may alter their stability [38]. Additionally, while nano-FTIR achieves superior spatial resolution (10–20 nm) compared to traditional FTIR, this resolution may still be insufficient for resolving very small or closely spaced features within phages (e.g., neck). Sensitivity is another concern, as the nanoscale size of phages can result in weak signals, reducing detection accuracy [39,40]. Furthermore, overlapping peaks in spectra from complex biological molecules may make it difficult to distinguish specific features, such as protein secondary structures or nucleic acids. Lastly, although designed to be non-destructive, nano-FTIR carries a risk of sample damage caused by the scanning probe, requiring careful optimization of parameters.

These limitations highlight the need for complementary approaches to enhance the utility of nano-FTIR in studying phages and other biological systems. For instance, combining nano-FTIR with biological assays (e.g., plaque assays) can provide functional insights into phage activity. High-resolution imaging techniques such as TEM can visualize

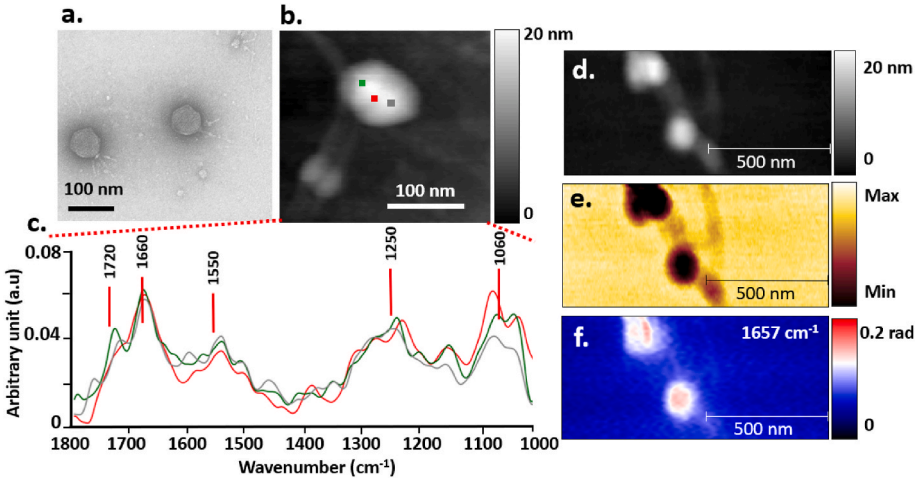

Fig. 2. (a) TEM image of PEV31 phages. (b) AFM height image of a single PEV31 and (c) its corresponding nano-FTIR spectra. (d) A second AFM height image of PEV31 and (e) the corresponding optical amplitude image. (f) Chemical map at 1657 cm^{-1} highlighting protein distribution.

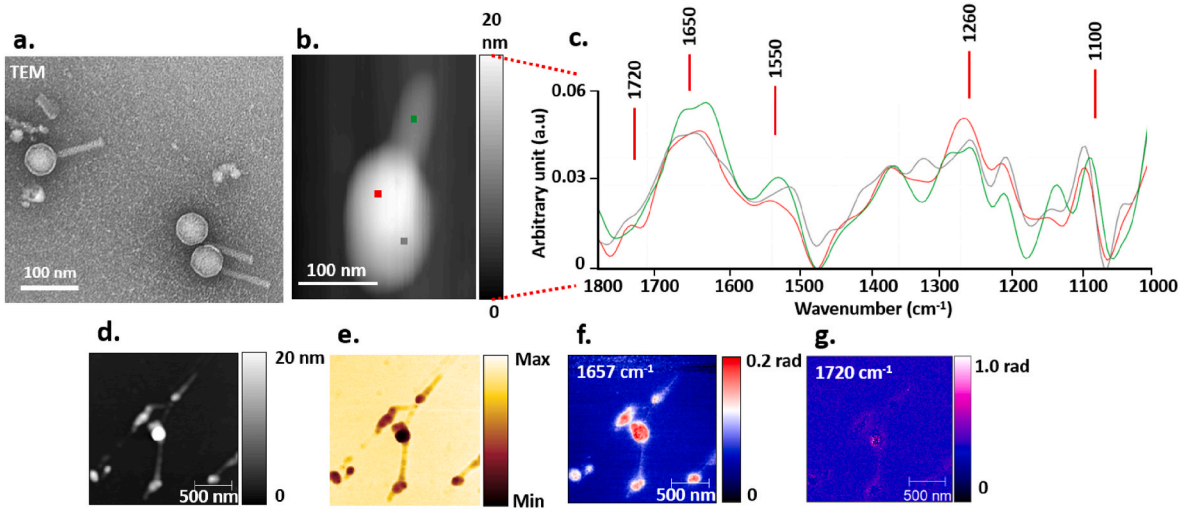

Fig. 3. (a) TEM image of PEV20 phages. (b) AFM height image of a single PEV20 and (c) the corresponding nano-FTIR spectrum acquired at different positions. (d) AFM height image of another PEV20, with (e) the corresponding optical amplitude image. (f) Chemical map at 1657 cm^{-1} highlighting protein distribution, and (g) map at 1720 cm^{-1} showing nucleic acid distribution.

fine morphological details of phages that are beyond the spatial resolution of nano-FTIR. Additionally, integrating genome sequencing can offer critical information about genetic materials, including genome structure and packaging mechanisms, which are essential for understanding phage biology [41].

4. Conclusion

Conventional techniques often fall short in detecting and analysing the protein-rich structures of phages due to their inadequate spatial resolution. Our approach using nano-FTIR overcomes this by revealing and spatially pinpointing the unique chemical signature of phages without changing their natural characteristics. Plaque assay can assess viable phages, but overlook those that are non-infectious, while TEM offers structural insights but fails to capture biochemical alterations. Nano-FTIR presents a novel method for comprehensive phage analysis, offering a precise chemical profiling at the nanoscale that traditional imaging lacks.

CRediT authorship contribution statement

Yue Cao: Writing – review & editing, Writing – original draft, Validation, Methodology, Investigation, Formal analysis, Data curation, Conceptualization. **Dipesh Khanal:** Writing – review & editing, Writing – original draft, Validation, Supervision, Methodology, Investigation, Formal analysis, Data curation, Conceptualization. **Adrian Cernescu:** Writing – review & editing, Validation. **Hak Kim Chan:** Writing – review & editing, Supervision, Project administration, Funding acquisition.

Declaration of generative AI and AI-assisted technologies in the writing process

Statement: During the preparation of this work the author(s) used [Chatgpt] in order to [improve the readability and language of the manuscript]. After using this tool/service, the author(s) reviewed and edited the content as needed and take(s) full responsibility for the content of the published article.

Declaration of competing interest

The authors declare that they have no known competing financial interests or personal relationships that could have appeared to influence the work reported in this paper.

Acknowledgement

This work was supported part by an ARC Discovery Project 210102526 to HKC and MMBH. The authors thank Dr. Elizabeth Kutter from the Evergreen Phage Lab, Washington, USA, for providing the phage stocks. The authors acknowledge the facilities and the scientific and technical assistance of Sydney Analytical and Sydney Microscopy & Microanalysis, a core research facility at The University of Sydney.

Data availability

Data will be made available on request.

References

[1] R.Y.K. Chang, M. Wallin, Y. Lin, S.S.Y. Leung, H. Wang, S. Morales, H.K. Chan, Phage therapy for respiratory infections, Adv. Drug Deliv. Rev. 133 (2018) 76–86, https://doi.org/10.1016/j.addr.2018.08.001.
[2] E. Jonczyk, M. Klak, R. Miedzybrodzki, A. Gorski, The influence of external factors on bacteriophages–review, Folia Microbiol. 56 (3) (2011) 191–200, https://doi.org/10.1007/s12223-011-0039-8.
[3] Y. Cao, D. Khanal, J. Kim, R.Y.K. Chang, A.S. Byun, S. Morales, M.M. Banaszak Holl, H.K. Chan, Stability of bacteriophages in organic solvents for formulations, Int. J. Pharm. 646 (2023) 123505, https://doi.org/10.1016/j.ijpharm.2023.123505.
[4] H.W. Ackermann, Bacteriophage observations and evolution, Res. Microbiol. 154 (4) (2003) 245–251, https://doi.org/10.1016/S0923-2508(03)00067-6.
[5] P. Zhvania, N.S. Hoyle, L. Nadareishvili, D. Nizharadze, M. Kutateladze, Phage therapy in a 16-Year-Old boy with Netherton Syndrome, Front Med-Lausanne 4 (2017) 94, https://doi.org/10.3389/fmed.2017.00094. ARTN 94.
[6] M. Zaczek, B. Weber-Dabrowska, R. Miedzybrodzki, M. Lusiak-Szelachowska, A. Górski, Phage therapy in Poland - a Centennial journey to the first ethically approved treatment facility in Europe, Front. Microbiol. 11 (2020) 1056, https://doi.org/10.3389/fmicb.2020.01056. ARTN 1056.
[7] P. Jault, T. Leclerc, S. Jennes, J.P. Pirnay, Y.A. Que, G. Resch, A.F. Rousseau, F. Ravat, H. Carsin, R. Le Floch, et al., Efficacy and tolerability of a cocktail of bacteriophages to treat burn wounds infected by (PhagoBurn): a randomised, controlled, double-blind phase 1/2 trial, Lancet Infect. Dis. 19 (1) (2019) 35–45, https://doi.org/10.1016/S1473-3099(18)30482-1.
[8] S.S.Y. Leung, N.B. Carrigy, R. Vehring, W.H. Finlay, S. Morales, E.A. Carter, W. J. Britton, E. Kutter, H.K. Chan, Jet nebulization of bacteriophages with different tail morphologies - structural effects, Int. J. Pharm. 554 (2019) 322–326, https://doi.org/10.1016/j.ijpharm.2018.11.026.
[9] M. Yamashita, H. Murahashi, T. Tomita, A. Hirata, Effect of alcohols on escherichia coil phages, Biocontrol Sci. 5 (1) (2000) 9–16, https://doi.org/10.4265/bio.5.9.
[10] R. Lavigne, P.J. Ceyssens, J. Robben, Phage proteomics: applications of mass spectrometry, Methods Mol. Biol. 502 (2009) 239–251, https://doi.org/10.1007/978-1-60327-565-1_14.

[11] I. Amenabar, S. Poly, W. Nuansing, E.H. Hubrich, A.A. Govyadinov, F. Huth, R. Krutokhvostov, L.B. Zhang, M. Knez, J. Heberle, et al., Structural analysis and mapping of individual protein complexes by infrared nanospectroscopy, Nat. Commun. 4 (2013), https://doi.org/10.1038/ncomms3890. ARTN 2890.
[12] S. Amarie, P. Zaslansky, Y. Kajihara, E. Griesshaber, W.W. Schmahl, F. Keilmann, Nano-FTIR chemical mapping of minerals in biological materials, Beilstein J. Nanotechnol. 3 (2012) 312–323, https://doi.org/10.3762/bjnano.3.35.
[13] F. H, A. G, S. A, W. N, F. K, R. H, Nano-FTIR absorption spectroscopy of molecular fingerprints at 20 nm spatial resolution, Nano Lett. 12 (8) (2012) 3973–3978.
[14] B. Pollard, E.A. Muller, K. Hinrichs, M.B. Raschke, Vibrational nano-spectroscopic imaging correlating structure with intermolecular coupling and dynamics, Nat. Commun. 5 (2014) 3587, https://doi.org/10.1038/ncomms4587.
[15] A. Dazzi, F. Glotin, R. Carminati, Theory of infrared nanospectroscopy by photothermal induced resonance, J. Appl. Phys. 107 (12) (2010), https://doi.org/10.1063/1.3429214. Artn 124519.
[16] A. Dazzi, R. Prazeres, E. Glotin, J.M. Ortega, Local infrared microspectroscopy with subwavelength spatial resolution with an atomic force microscope tip used as a photothermal sensor, Opt Lett. 30 (18) (2005) 2388–2390, https://doi.org/10.1364/Ol.30.002388.
[17] J. Houel, E. Homeyer, S. Sauvage, P. Boucaud, A. Dazzi, R. Prazeres, J.M. Ortéga, Midinfrared absorption measured at a λ/400 resolution with an atomic force microscope, Opt. Express 17 (13) (2009) 10887–10894, https://doi.org/10.1364/Oe.17.010887.
[18] P.M. Donaldson, C.S. Kelley, M.D. Frogley, J. Filik, K. Wehbe, G. Cinque, Broadband near-field infrared spectromicroscopy using photothermal probes and synchrotron radiation, Opt. Express 24 (3) (2016) 1852–1864, https://doi.org/10.1364/Oe.24.001852.
[19] D. Khanal, R.Y.K. Chang, S. Morales, H.K. Chan, W. Chrzanowski, High resolution nanoscale probing of bacteriophages in an inhalable dry powder formulation for pulmonary infections, Anal. Chem. 91 (20) (2019) 12760–12767, https://doi.org/10.1021/acs.analchem.9b02282.
[20] V. Stanic, F.C.B. Maia, R.O. Freitas, F.E. Montoro, K. Evans-Lutterodt, The chemical fingerprint of hair melanosomes by infrared nano-spectroscopy, Nanoscale 10 (29) (2018) 14245–14253, https://doi.org/10.1039/c8nr03146k.
[21] A. Cernescu, M. Szuwarzynski, U. Kwolek, P. Wydro, M. Kepczynski, S. Zapotoczny, M. Nowakowska, L. Quaroni, Correction to label-free infrared spectroscopy and imaging of single phospholipid bilayers with nanoscale resolution, Anal. Chem. 93 (3) (2021) 1851, https://doi.org/10.1021/acs.analchem.0c04696.
[22] A. Blat, J. Dybas, M. K, K. C, K. B, R.B. K, A. C, K. M, K.M. Marzec, An analysis of isolated and intact RBC membranes — a comparison of a semiquantitative approach by means of FTIR, nano-FTIR and raman spectroscopies, Anal. Chem. 91 (2019) 9867.
[23] L.R. de Mello, I.W.C.V. Hamley, B.B.M. Garcia, S.W. Han, C.L.P. de Oliveira, E. R. da Silva, Nanoscopic structure of complexes formed between DNA and the cell-penetrating peptide penetratin, J. Phys. Chem. B 123 (42) (2019) 8867–8871, https://doi.org/10.1021/acs.jpcb.9b05512.
[24] T. Dou, Z. Li, J. Zhang, A. Evilevitch, D. Kurouski, Nanoscale structural characterization of individual viral particles using atomic force microscopy infrared spectroscopy (AFM-IR) and tip-enhanced raman spectroscopy (TERS), Anal. Chem. 92 (16) (2020) 11297–11304, https://doi.org/10.1021/acs.analchem.0c01971.
[25] F. Huth, A. Govyadinov, S. Amarie, W. Nuansing, F. Keilmann, R. Hillenbrand, Nano-FTIR absorption spectroscopy of molecular fingerprints at 20 nm spatial resolution, Nano Lett. 12 (8) (2012) 3973–3978, https://doi.org/10.1021/nl301159v.
[26] H. Yue, Y. Li, M.Y. Yang, C.B. Mao, T7 phage as an emerging nanobiomaterial with genetically tunable target specificity, Adv. Sci. 9 (4) (2022), https://doi.org/10.1002/advs.202103645. ARTN 2103645.
[27] P. Kemp, L.R. Garcia, I.J. Molineux, Changes in bacteriophage T7 virion structure at the initiation of infection, Virology 340 (2) (2005) 307–317, https://doi.org/10.1016/j.virol.2005.06.039.
[28] V.B. Rao, A. Fokine, Q.L. Fang, Q.Q. Shao, Bacteriophage T4 head: structure, assembly, and genome packaging, Viruses 15 (2) (2023), https://doi.org/10.3390/v15020527. ARTN 527.
[29] S. Kanamaru, N.C. Gassner, N.Z. Ye, S. Takeda, F. Arisaka, The C-terminal fragment of the precursor tail lysozyme of bacteriophage T4 stays as a structural component of the baseplate after cleavage, J. Bacteriol. 181 (9) (1999) 2739–2744, https://doi.org/10.1128/Jb.181.9.2739-2744.1999.
[30] Y. Cao, D. Khanal, J. Kim, R.Y.K. Chang, A.S. Byun, S. Morales, M.M. Banaszak Holl, H.K. Chan, Stability of bacteriophages in organic solvents for formulations, Int. J. Pharm. 646 (2023) 123505, https://doi.org/10.1016/j.ijpharm.2023.123505.
[31] T. Eissa, L. Voronina, M. Huber, F. Fleischmann, M. Zigman, The perils of molecular interpretations from vibrational spectra of complex samples, Angew Chem. Int. Ed. Engl. 63 (50) (2024) e202411596, https://doi.org/10.1002/anie.202411596.
[32] N. Bonilla, M.I. Rojas, G. Netto Flores Cruz, S.H. Hung, F. Rohwer, J.J. Barr, Phage on tap-a quick and efficient protocol for the preparation of bacteriophage laboratory stocks, PeerJ 4 (2016) e2261, https://doi.org/10.7717/peerj.2261.
[33] D.J. Malik, I.J. Sokolov, G.K. Vinner, F. Mancuso, S. Cinquerrui, G. T. Vladisavljevic, M.R.J. Clokie, N.J. Garton, A.G.F. Stapley, A. Kirpichnikova, Formulation, stabilisation and encapsulation of bacteriophage for phage therapy, Adv. Colloid Interface Sci. 249 (2017) 100–133, https://doi.org/10.1016/j.cis.2017.05.014.
[34] K. Kochan, C. Nethercott, D. Perez Guaita, J.H. Jiang, A.Y. Peleg, B.R. Wood, P. Heraud, Detection of antimicrobial resistance-related changes in biochemical composition of Staphylococcus aureus by means of atomic force microscopy-infrared spectroscopy, Anal. Chem. 91 (24) (2019) 15397–15403, https://doi.org/10.1021/acs.analchem.9b01671.
[35] N.D. Seeley, S.B. Primrose, The isolation of bacteriophages from the environment, J. Appl. Bacteriol. 53 (1) (1982) 1–17, https://doi.org/10.1111/j.1365-2672.1982.tb04729.x.
[36] A. Bruttin, H. Brüssow, Human volunteers receiving phage T4 orally:: a safety test of phage therapy, Antimicrob. Agents Chemother. 49 (7) (2005) 2874–2878, https://doi.org/10.1128/Aac.49.7.2874-2878.2005.
[37] E. Kutter, D. De Vos, G. Gvasalia, Z. Alavidze, L. Gogokhia, S. Kuhl, S.T. Abedon, Phage therapy in clinical practice: treatment of human infections, Curr. Pharm. Biotechnol. 11 (1) (2010) 69–86, https://doi.org/10.2174/138920110790725401.
[38] M. Wdowiak, J. Paczesny, S. Raza, Enhancing the stability of bacteriophages using physical, chemical, and nano-based approaches: a review, Pharmaceutics 14 (9) (2022) 1936, https://doi.org/10.3390/pharmaceutics14091936.
[39] Z. Aliakbar Ahovan, A. Hashemi, L.M. De Plano, M. Gholipourmalekabadi, A. Seifalian, Bacteriophage based biosensors: trends, outcomes and challenges, Nanomaterials 10 (3) (2020), https://doi.org/10.3390/nano10030501.
[40] A. Singh, S.K. Arya, N. Glass, P. Hanifi-Moghaddam, R. Naidoo, C.M. Szymanski, J. Tanha, S. Evoy, Bacteriophage tailspike proteins as molecular probes for sensitive and selective bacterial detection, Biosens. Bioelectron. 26 (1) (2010) 131–138, https://doi.org/10.1016/j.bios.2010.05.024.
[41] J.C.A. Friedersdorff, A.H. Kingston-Smith, J.A. Pachebat, A.R. Cookson, D. Rooke, C.J. Creevey, The isolation and genome sequencing of five novel bacteriophages from the rumen active against Butyrivibrio fibrisolvens, Front. Microbiol. 11 (2020) 1588, https://doi.org/10.3389/fmicb.2020.01588.